Articles

Xanthene-Phosphole Ligands: Synthesis, Coordination Chemistry, and Activity in the Palladium-Catalyzed Amine Allylation

Guilhem Mora, Bernard Deschamps, Steven van Zutphen, Xavier F. Le Goff, Louis Ricard, and Pascal Le Floch*

Laboratoire "Hétéroéléments et Coordination", Ecole Polytechnique, CNRS, 91128 Palaiseau Cédex, France

Received December 22, 2006

Two new xanthene-phosphole derivatives, **3** and **4**, were synthesized through the nucleophilic substitution of the cyano group in 1-*P*-cyano-2,5-diphenylphosphole (**1**) and 1-*P*-cyano-3,4-dimethylphosphole (**2**) by the 4,5-dilithium salt of 9,9′-dimethylxanthene. For this, a new synthetic procedure was developed, allowing the synthesis of the required 1-*P*-cyano-2,5-diphenylphosphole from the 1,2,5-triphenylphosphole. Both ligands (DPP-Xantphos **3** for the diphenyl derivative and DMP-Xantphos **4** for the dimethyl derivative) react with $[Pd(allyl)Cl]_2$ to afford the corresponding cationic complexes **5Cl** and **6Cl**. Using AgOTf, stable triflate complexes **5OTf** and **6OTf** could be isolated. The chloride complexes, on the other hand, exhibit a limited stability in solution. The DPP-Xantphos derivative **5Cl** eliminates allyl chloride to yield the dimeric palladium(0) complex **7** of general formula $[Pd(\mathbf{3})]_2$, in which each palladium is coordinated to the two phosphorus atoms of the same ligand and to one double bond of one phosphole unit of the second ligand. Decomposition of complex **6Cl** furnished a mixture of compounds featuring a dimeric trinuclear species of general formula $[Pd_3(\mathbf{4})_2Cl_2]$. This complex was also synthesized directly. Reaction of the DMP-Xantphos ligand **4** with 1 equiv of $[Pd(COD)Cl_2]$ and 2 equiv of $[Pd(dba)_2]$ afforded dimer **8**, which features one 18-VE Pd^0 center and two Pd-Cl fragments, which are coordinated to the dienic system of the two phosphole ligands and connected through a single Pd−Pd bond. The catalytic activity of the triflate complexes **5OTf** and **6OTf** was evaluated in the allylation of aniline. Whereas the DMP-Xantphos derivative **6OTf** exhibited a poor catalytic activity, very good conversion yields were obtained with the DPP-Xantphos complex **5OTf**. On the basis of X-ray structure data and DFT calculations, it was concluded that the high catalytic activity of the DPP-Xantphos derivative complex [Pd(allyl)**3**][OTf] (**6OTf**) results from the combination of two effects: a large P−Pd−P bite angle, which enhances the reactivity of the allyl ligand, and the strong π-accepting capacity of the diphenylphosphole moiety, which allows the easy formation of a 14-VE complex.

Introduction

The combination of electronic and steric effects plays a crucial role in the fine-tuning of a catalyst's activity and selectivity. This is particularly true for phosphine-based ligands, widely used in many catalytic transformations of synthetic relevance. In the case of diphosphine ligands, a third parameter, the bite angle, needs to be considered.[1−5] Various recent studies have unambiguously shown that even small variations of this parameter often result in dramatic changes in a catalyst's activity and stereoselectivity. Illustrative examples are given by hydroformylation,[6] hydrocyanation,[7] and alkylation or amination reactions.[8−11] In general, to investigate the ideal bite angle, one can employ rigid aromatic backbones containing easily functionalizable sites. Such a strategy has been nicely exploited by Van Leeuwen and his group in the case of xanthene derivatives (Scheme 1).[12−20] Xantphos derivatives, consisting of a xanthene skeleton with two acyclic or cyclic phosphine ligands, have thus

* Corresponding author. Tel: +33 1 69 33 45 70. Fax: +33 1 69 33 39 90. E-mail: lefloch@poly.polytechnique.fr.

(1) For a review on the effect of the ligand bite angle, see: van Leeuwen, P. W. N. M.; Kamer, P. C. J.; Reek, J. N. H.; Dierkes, P. *Chem. Rev.* **2000**, *100*, 2741−2770.

(2) Casey, C. P.; Whiteker, G. T. *Isr. J. Chem.* **1990**, *30*, 299.

(3) Freixa, Z.; van Leeuwen, P. W. N. M. *Dalton Trans.* **2003**, 1890−1901.

(4) van Leeuwen, P. W. N. M.; Kamer, P. C. J.; Reek, J. N. H. *Pure Appl. Chem.* **1999**, *8*, 1443.

(5) Dierkes, P.; van Leeuwen, P. W. N. M. *J. Chem. Soc., Dalton Trans.* **1999**, 1519−1529.

(6) Kranenburg, M.; van der Burgt, Y. E. M.; Kamer, P. C. J.; van Leeuwen, P. W. N. M.; Goubitz, K.; Fraanje, J. *Organometallics* **1995**, *14*, 3081−3089.

(7) Goertz, W.; Keim, W.; Vogt, D.; Englert, U.; Boele, M. D. K.; van der Veen, L. A.; Kamer, P. C. J.; van Leeuwen, P. W. N. M. *J. Chem. Soc., Dalton Trans.* **1998**, 2981−2988.

(8) van Haaren, R. J.; Goubitz, K.; Fraanje, J.; van Strijdonck, G. P. F.; Oevering, H.; Coussens, B.; Reek, J. N. H.; Kamer, P. C. J.; van Leeuwen, P. W. N. M. *Inorg. Chem.* **2001**, *40*, 3363−3372.

(9) Johns, A. M.; Utsunomiya, M.; Incarvito, C. D.; Hartwig, J. F. *J. Am. Chem. Soc.* **2006**, *128*, 1828−1839.

(10) Kranenburg, M.; van der Burgt, Y. E. M.; Kamer, P. C. J.; van Leeuwen, P. W. N. M. *Eur. J. Inorg. Chem.* **1998**, 155−157.

(11) Kranenburg, M.; Kamer, P. C. J.; van Leeuwen, P. W. N. M. *Eur. J. Inorg. Chem.* **1998**, 25−27.

(12) Bronger, R. P. J.; Bermon, J. P.; Herwig, J.; Kamer, P. C. J.; van Leeuwen, P. W. N. M. *Adv. Synth. Catal.* **2004**, *346*, 789−799.

10.1021/om061172t CCC: $37.00
Publication on Web 03/16/2007

Scheme 1. General Formula of Xantphos Derivatives

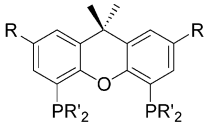

dimethyl xantphos derivatives

found important applications in processes, including the linear hydroformylation of alkenes, where the selectivity was shown to be highly dependent on the P−Rh−P bite angle.[6,19]

In the current work we report the synthesis of two new xantphos derivatives featuring phospholes, their coordination chemistry, including their palladium allyl complexes, and their catalytic activities in amine allylation reactions. Phospholes, unsaturated phosphorus-containing five-membered heterocycles, exhibit a very rich chemistry, making them attractive building blocks for a wide variety of purposes including serving as ligands in catalysis.[21,22] This study was motivated by two recent findings. First, we found that phosphole derivatives can be successfully applied to palladium-catalyzed allylation reactions of primary amines.[23] Using DFT calculations we proved that the rate-limiting step in this catalysis is highly dependent on the nature of the phosphine ligand and that the best results are obtained with strong π-acceptor ligands such as phospholes.[24] Second, Hartwig and co-workers showed that diphosphines with a large bite angle surrounding a palladium allyl complex favor nucleophilic attack of amines onto η^3-allyl and η^3-benzyl complexes.[9] We reasoned that xantphos derivatives featuring phospholes would give rise to strongly π-accepting ligands with a large bite angle and thus be of interest for the catalysis of amine allylations.

Results and Discussion

1. Syntheses of DPP and DMP-Xantphos Ligands 3 and 4. Two differently substituted phospholes were selected for our experiments: the readily available 2,5-diphenyl (DPP) and 3,4-dimethyl (DMP) phospholes. Synthesis of xanthene derivatives featuring phospholes is not unprecedented; two examples were already reported by van Leeuwen and his group with tetraphenylphosphole (TPP-Xantphos) and with dibenzophosphole (DBP-xantphos).[20] These were synthesized by reacting the 4,5-dilithium salt of xanthene with the corresponding chlorophosphine. Although both chloro and bromo derivatives of 2,5-diphenylphosphole and 3,4-dimethylphosphole are available, they are very reactive and difficult to handle.[25] We therefore decided to use the corresponding P-cyano phospholes, 1-cyano-2,5-diphenylphosphole (**1**) and 1-cyano-3,4-dimethylphosphole (**2**). The synthesis of phosphole **2** has been described in the literature, and it was easily prepared in high yield.[26] On the other hand, phosphole **1** had not been synthesized before. We found that it could be readily prepared following the same procedure, which consists of reacting the phospholide anion with cyanogen bromide at low temperature in THF. After workup and purification, phosphole **1** was recovered as a yellow powder in 70% yield (Scheme 2).

Scheme 2. Synthesis of the Cyanophosphole 1

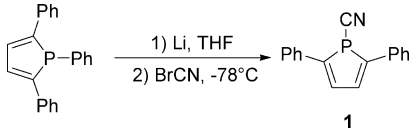

1

Scheme 3. Synthesis of DPP- and DMP-Xantphos Derivatives 3 and 4

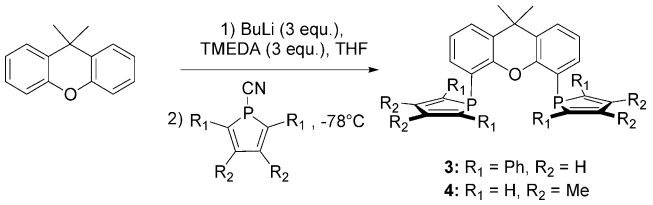

3: R_1 = Ph, R_2 = H
4: R_1 = H, R_2 = Me

Reaction of the 4,5-dilithium salt of 9,9′-dimethylxanthene with phospholes **1** and **2** at low temperature in THF afforded the corresponding DPP-Xantphos **3** and DMP-Xantphos **4** in acceptable yields (>50%) (Scheme 3). The diphosphines **3** and **4** were isolated as an air-stable yellow and white solid, respectively. They were fully characterized by conventional NMR techniques (^{31}P, ^{1}H, and ^{13}C), mass spectrometry, and elemental analysis.

Additionally the structure of compound **3** was confirmed by an X-ray crystal structure analysis. A view of one molecule of **3** is presented in Figure 1, and the most significant parameters are listed in the corresponding legend. Crystal data and structural refinement details are presented in Table 1. The structure of **3** deserves no further comments, with all bond lengths and bond angles comparable to those of classical xantphos[6] and 1-P-substituted diphenylphosphole derivatives.[27−30]

2. Syntheses of Palladium(allyl) and Palladium(0) Complexes of Ligands 3 and 4. Reactivity of **3** and **4** toward the $[Pd(allyl)Cl]_2$ dimer was investigated. In both cases a clean reaction takes place in dichloromethane at room temperature in the presence of AgOTf as chloride abstractor to afford complexes **5OTf** and **6OTf**. The complexes were obtained as yellow-green and white-gray powders, respectively (Scheme 4).

Both complexes were fully characterized by NMR techniques (^{31}P, ^{1}H, ^{13}C), mass spectrometry, elemental analysis, and X-ray

(13) Bronger, R. P. J.; Bermon, J. P.; Reek, J. N. H.; Kamer, P. C. J.; van Leeuwen, P. W. N. M.; Carter, D. N.; Licence, P.; Poliakoff, M. *J. Mol. Catal. A Chem.* **2004**, *224*, 145−152.
(14) Chen, R.; Bronger, R. P. J.; Kamer, P. C. J.; van Leeuwen, P. W. N. M.; Reek, J. N. H. *J. Am. Chem. Soc.* **2004**, *126*, 14557−14566.
(15) Bronger, R. P. J.; Silva, S. M.; Kamer, P. C. J.; van Leeuwen, P. W. N. M. *Dalton Trans.* **2004**, 1590−1596.
(16) Bronger, R. P. J.; Silva, S. M.; Kamer, P. C. J.; van Leeuwen, P. W. N. M. *Chem. Commun.* **2002**, 3044−3045.
(17) Kamer, P. C. J.; van Leeuwen, P. W. N. M.; Reek, J. N. H. *Acc. Chem. Res.* **2001**, *34*, 895−904.
(18) Carbo, J. J.; Maseras, F.; Bo, C.; van Leeuwen, P. W. N. M. *J. Am. Chem. Soc.* **2001**, *123*, 7630 −7637.
(19) van der Veen, L. A.; Keeven, P. H.; Schoemaker, G. C.; Reek, J. N. H.; Kamer, P. C. J.; van Leeuwen, P. W. N. M.; Lutz, M.; Spek, A. L. *Organometallics* **2000**, *19*, 872−883.
(20) van der Veen, L. A.; Kamer, P. C. J.; van Leeuwen, P. W. N. M. *Organometallics* **1999**, *18*, 4765−4777.
(21) Quin, L. D. In *Phosphorus-Carbon Heterocyclic Chemistry: The Rise of a New Domain*; Mathey, F., Ed.; Pergamon: Amsterdam, 2001; p 219.
(22) Mathey F. In *Phosphorus-Carbon Heterocyclic Chemistry: The Rise of a New Domain*; Mathey, F.. Ed.; Pergamon: Amsterdam, 2001; p 753.
(23) Thoumazet, C.; Grutzmacher, H.; Deschamps, B.; Ricard, L.; le Floch, P. *Eur. J. Inorg. Chem.* **2006**, *19*, 3911−3922.
(24) Piechaczyk, O.; Thoumazet, C.; Jean, Y.; le Floch, P. *J. Am. Chem. Soc.* **2006**, *128*, 14306−14317.
(25) Charrier, C.; Bonnard, H.; Mathey, F.; Neibecker, D. *J. Organomet. Chem.* **1982**, *231*, 361−367.
(26) Holand, S.; Mathey, F. *Organometallics* **1988**, *7*, 1796−1801.
(27) Mora, G.; van Zutphen, S.; Thoumazet, C.; Le Goff, X. F.; Ricard, L.; Grützmacher, H.; Le Floch, P. *Organometallics* **2006**, *25*, 5528−5532.
(28) Thoumazet, C.; Ricard, L.; Grutzmacher, H.; le Floch, P. *Chem. Commun.* **2005**, 1592−1594.
(29) Thoumazet, C.; Melaimi, M.; Ricard, L.; Mathey, F.; le Floch, P. *Organometallics* **2003**, *22*, 1580−1581.
(30) Melaimi, M.; Thoumazet, C.; Rocard, L.; le Floch, P. *J. Organomet. Chem.* **2004**, *689*, 2988−2994.

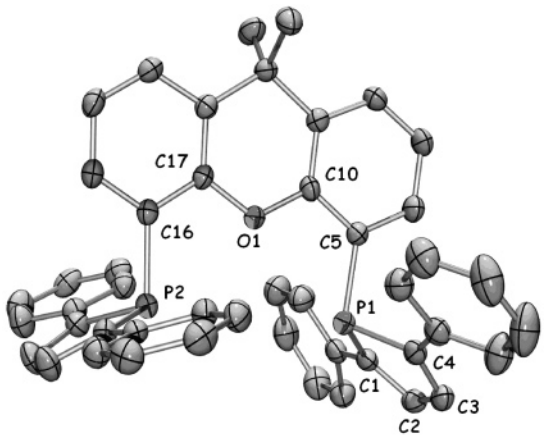

Figure 1. View of one molecule of **3**. The numbering is arbitrary and different from that used in NMR spectra. Thermal ellipsoids are drawn at the 30% probability level. Hydrogen atoms are omitted for clarity. Selected bond distances (Å) and angles (deg): P(1)−C(1), 1.808(2); C(1)−C(2), 1.364(2); C(2)−C(3), 1.433(2); C(3)−C(4), 1.367(2); P(1)−C(4), 1.807(2); P(1)−C(5), 1.830(2); C(5)−C(10), 1.401(2); O(1)−C(10), 1.377(2); O(1)−C(17), 1.386(2); C(16)−C(17), 1.394(2); P(2)−C(16), 1.836(2); C(1)−P(1)−C(5), 107.02(7); C(4)−P(1)−C(5), 103.28(7); C(4)−P(1)−C(1), 91.88(7); C(2)−C(1)−P(1), 107.6(1); C(1)−C(2)−C(3), 115.6(2); C(4)−C(3)−C(2), 114.9(2); C(3)−C(4)−P(1), 107.9(1); C(10)−C(5)−P(1), 119.4(1); O(1)−C(10)−C(5), 114.6(1); C(10)−O(1)−C(17), 119.8(1); O(1)−C(17)−C(16), 114.7(1); C(17)−C(16)−P(2), 120.7(1).

Table 1. Crystal Data and Structural Refinement Details for 3

cryst size [mm]	0.22 × 0.16 × 0.10
empirical formula	$C_{47}H_{36}OP_2$
molecular mass	678.70
cryst syst	lemon yellow plate
space group	$P2_1/c$
a [Å]	11.819(1)
b [Å]	17.351(1)
c [Å]	17.584(1)
α [deg]	90.00
β [deg]	101.065(1)
γ [deg]	90.00
V [Å]^3	3538.9(4)
Z	4
calcd density [g·cm^{-3}]	1.274
abs coeff [cm^{-1}]	0.160
θ_{max} [deg]	27.47
F(000)	1424
index ranges	−15 15; −22 20; −22 22
no. of reflns collected/indep	14 286/8085
no. of reflns used	5733
R_{int}	0.0267
abs corr	0.9657 min., 0.9842 max.
no. of params refined	454
refln/param	12
final R1[a]/wR2 [$I > 2\sigma(I)$][b]	0.0412/0.1163
goodness-of-fit on F^2	1.030
diff peak/hole [e·Å^{-3}]	0.286(0.045)/−0.287(0.045)

[a] $R1 = \Sigma||F_o| - |F_c||/\Sigma|F_o|$. [b] $wR2 = (\Sigma w||F_o| - |F_c||^2/\Sigma w|F_o|^2)^{1/2}$.

crystallography. Views of a single molecule of **5OTf** and **6OTf** are presented in Figures 2 and 3, respectively, and the most significant metric parameters are listed in the corresponding legends. Crystal data and structural refinement details are presented in Table 2.

In both structures, the palladium environment formed by the two phosphorus atoms and the allyl fragment is square planar. However, the orientation of this plane (P1, Scheme 5) relative to the mean plane of the ligand defined by the two phosphorus atoms and the two quaternary carbon atoms bearing them (P2,

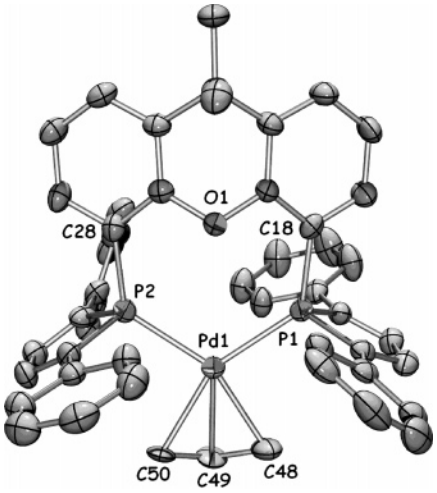

Figure 2. View of one molecule of **5OTf**. The numbering is arbitrary and different from that used in NMR spectra. Thermal ellipsoids are drawn at the 30% probability level. Hydrogen atoms are omitted for clarity. Selected bond distances (Å) and angles (deg): C(48)−C(49), 1.3600(1); C(49)−C(50), 1.3600(2); Pd(1)−C(48), 2.175(7); Pd(1)−C(49), 2.167(6); Pd(1)−C(50), 2.21(1); Pd(1)−P(1), 2.332(1); Pd(1)−P(2), 2.338(1); P(1)−C(18), 1.825(5); P(2)−C(28), 1.820(5); P(1)−Pd(1)−P(2), 116.08(4); C(49)−Pd(1)−P(1), 121.4(2); C(49)−Pd(1)−P(2), 120.7(2); C(28)−P(2)−Pd(1), 128.9(2); C(18)−P(1)−Pd(1), 128.3(2).

Scheme 4. Synthesis of Palladium Allyl Complexes 5OTf and 6OTf

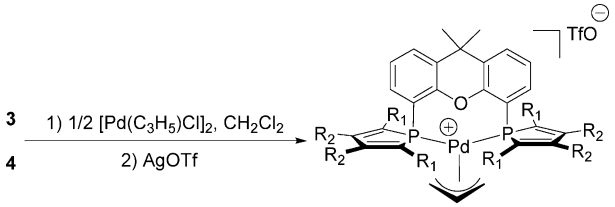

5: R_1 = Ph, R_2 = H
6: R_1 = H, R_2 = Me

Scheme 5) differs greatly in the two structures. We can define Θ as the angle between the plane P1 and the plane P2. Whereas the Pd nearly lies in the same plane as the xanthene in the case of complex **5OTf** (Θ = 175.7°), it is nearly perpendicular to this plane in complex **6OTf** (Θ = 114.0°).

As illustrated in Figure 4, where a view of **5OTf** and **6OTf** are presented, the relative distortions are the direct result of the different substitution patterns of the phosphole rings. In **5OTf**, the "planar conformation" of the palladium allyl fragment relative to the xanthene allows the reduction of steric crowding between the phenyl groups on the adjacent phospholes. In **6OTf**, the ortho-positions of the phospholes are unsubstituted and the phosphole rings can freely rotate around the xanthene−P bond to adopt the most stable conformation, pushing the palladium allyl out of the plane P1. Note that a similar distortion is observed in other xantphos complexes: in the diphenylphosphino derivative, where steric crowding between the phenyl groups is expected, though probably to a lesser extent than in **5OTf**, Θ is found to be 137.9°.[9] A direct consequence of the distortion of **5OTf** with respect to **6OTf** is the widening of the P−Pd−P bite angle (α) in complex **5OTf** (α = 116.08(4)°) compared to **6OTf** (α = 103.39(3)°) or xantphos (α = 108.11(1)° with OTf as counterion[8]). As will be discussed later, this difference accounts for the relatively higher reactivity of **5OTf** toward nucleophiles.

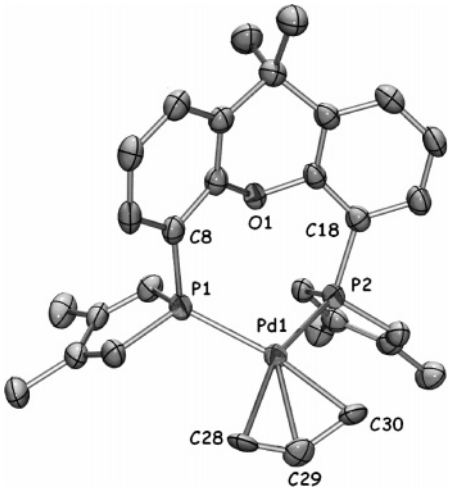

Figure 3. View of one molecule of **6OTf**. The numbering is arbitrary and different from that used in NMR spectra. Thermal ellipsoids are drawn at the 30% probability level. Hydrogen atoms are omitted for clarity. Selected bond distances (Å) and angles (deg): C(28)−C(29), 1.26(2); C(29)−C(30), 1.41(4); Pd(1)−C(28), 2.24(2); Pd(1)−C(29), 2.179(8); Pd(1)−C(30), 2.13(4); Pd(1)−P(1), 2.313(1); Pd(1)−P(2), 2.3247(8); P(1)−C(8), 1.830(3); P(2)−C(18), 1.815(3); C(29)−Pd(1)−P(1), 127.9(2); C(29)−Pd(1)−P(2), 127.3(2); P(1)−Pd(1)−P(2), 103.39(3); C(8)−P(1)−Pd(1), 113.1(1); C(18)−P(2)−Pd(1), 114.8(1).

Scheme 5. Out-of-Plane Displacement of the Ally Ligand in Complexes 5 and 6

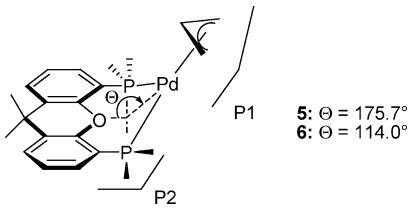

Scheme 6. Three Syntheses of Dimer 7

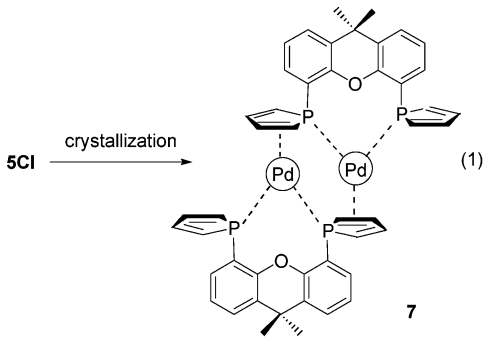

phenyl groups at phosphole were omitted for clarity

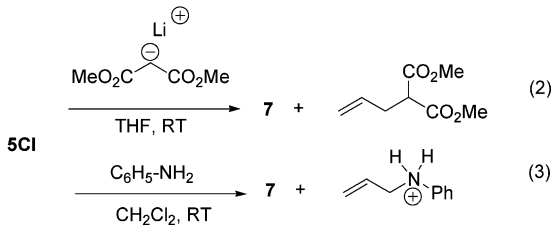

Additional experiments were carried out to synthesize cationic complexes of ligands **3** and **4** with different counteranions. A surprising result was obtained when no chloride abstractor was used. Reaction of ligands **3** and **4** with the $[Pd(allyl)Cl]_2$ dimer in dichloromethane at room temperature cleanly afforded complexes **5Cl** and **6Cl**. Both complexes were isolated as yellow and white powders, respectively, and characterized by ^{31}P NMR spectroscopy. Their chemical shifts were found to be similar to that of their triflate counterparts, confirming their structural similarity. However, both species exhibit a moderate stability in solution, and within a few hours additional signals around 15 ppm appear in the ^{31}P NMR spectra, which could not be assigned directly. Several attempts were made to crystallize the two chloride complexes. Whereas complex **6Cl**, or its decomposition products, could not be crystallized, diffusion of petroleum ether into a dichloromethane solution of complex **5Cl** at room temperature afforded dark red crystals of complex **7** (Scheme 6, eq 1). A view of one molecule of complex **7** is presented in Figure 5, and the most significant metric parameters are listed in the corresponding legend. Crystal data and structural refinement details are presented in Table 3.

As can be seen, complex **7** is not the expected cationic palladium allyl species, but a 32-VE dimeric palladium(0) complex featuring two [(DPP-Xantphos)Pd^0] fragments. Each DPP-xantphos ligand (**3**) behaves as a six-electron donor. Four electrons are donated by the two phosphorus atoms bound to the same palladium atom, while two additional electrons are donated to the second palladium atom by one double bond of one phosphole ligand through η^2-coordination. Each palladium atom adopts a nearly trigonal planar geometry, as expected for a d^{10} PdL_3 complex. It is probably due to geometrical constraints that the two phosphorus−palladium bond lengths are slightly different (d(P1−Pd1) = 2.309(1) Å and d(P2−Pd1) = 2.335(1) Å). Another interesting piece of data is the C═C bond lengths of the phosphole moieties. Indeed, a strong π-back-bonding occurs with the [Pd(**3**)] fragment. As a result, the coordinated double bond is significantly lengthened (1.435(4) vs 1.343(5) Å for the uncoordinated bond).

Complex **7** was also identified by elemental analysis, but its high insolubility precluded the recording of ^{31}P, ^{1}H, and ^{13}C NMR spectra. The mechanism of formation of **7** could not be established with accuracy, but one may propose that it relies on the transient formation of a 14-VE [Pd(**3**)] complex, which subsequently dimerizes. The only way to rationalize formation of this unsaturated species is to consider that the chloride counteranion behaves as a nucleophile onto the allyl fragment, allowing the release of allyl chloride. To verify this hypothesis, complex **5Cl** was reacted with both lithium malonate dimethyl ester and aniline at room temperature (Scheme 6, eqs 2 and 3). Either reaction occurred readily, leading to the formation of complex **7** as a dark red powder. The formulation of these powders was confirmed by elemental analysis and X-ray analysis. Indeed slow diffusion of a solution of aniline in hexane into a dichloromethane solution of complex **5Cl** yielded crystals of **7** (analogous to those recorded previously). Note that the same results were obtained when reactions were carried out on the **5OTf** derivative.

In pursuing our investigations we found that complex **6Cl** exhibited a totally different reactivity when carrying out the same reaction under the same experimental conditions. Addition of lithium malonate dimethyl ester to a solution of **6Cl** yielded a complex mixture of compounds whose structures could not be established on the sole basis of the ^{31}P NMR spectrum. Careful examination of the spectrum of this crude mixture, however, revealed the presence of a major compound, **8**, which exhibited a AA′BB′ spin system pattern. Fortunately single crystals of this complex could be grown by slow diffusion of petroleum ether into the crude mixture. A view of complex **8**

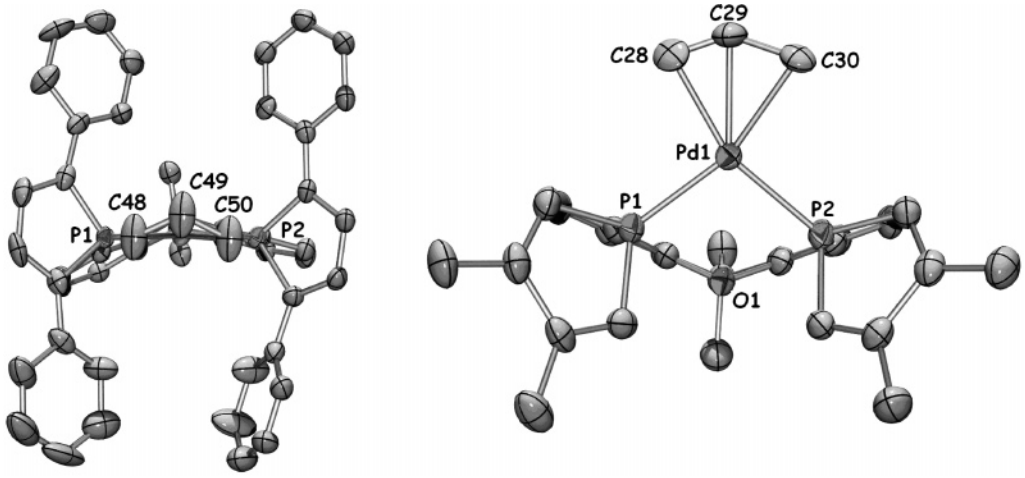

Figure 4. Views of complexes **5OTf** (left) and **6OTf** (right) showing the relative position of the palladium allyl fragments toward the mean plane of the complex.

Table 2. Crystal Data and Structural Refinement Details for 5OTf and 6OTf

	5OTf	6OTf
cryst size [mm]	0.16 × 0.04 × 0.04	0.40 × 0.12 × 0.02
empirical formula	$2(C_{50}H_{41}OP_2Pd)_2(CF_3O_3S)CH_2Cl_2$	$C_{30}H_{33}OP_2PdCF_3O_3S2(CH_2Cl_2)$
molecular mass	2120.33	896.83
cryst syst	monoclinic	orthorhombic
space group	$P2_1/c$	*Pbca*
a [Å]	11.186(1)	15.022(1)
b [Å]	55.192(1)	20.250(1)
c [Å]	15.304(1)	24.550(1)
α [deg]	90.00	90.00
β [deg]	97.412(1)	90.00
γ [deg]	90.00	90.00
V [Å]^3	9369.4(11)	7468.0(7)
Z	4	8
calcd density [g·cm^{-3}]	1.503	1.595
abs coeff [cm^{-1}]	0.681	0.976
θ_{max} [deg]	26.37	27.48
F(000)	4320	3632
index ranges	−13 11; −63 68; −14 19	−19 15; −24 24; −25 31
no. of reflns collected/indep	51 275/17 259	28 071/8226
no. of reflns used	13 013	5573
R_{int}	0.0345	0.0370
abs corr	0.8988 min., 0.9733 max.	0.6962 min., 0.9807 max.
no. of params refined	1138	434
reflection/param	11	12
final R1[a]/*w*R2 [$I > 2\sigma(I)$][b]	0.0614/0.2128	0.0429/0.1241
goodness-of-fit on F^2	1.132	1.005
diff peak/hole [e·Å^{-3}]	0.966(0.132)/−1.083(0.132)	1.221(0.084)/−0.618(0.084)

[a] $R1 = \sum||F_o| - |F_c||/\sum|F_o|$. [b] $wR2 = (\sum w||F_o| - |F_c||^2/\sum w|F_o|^2)^{1/2}$.

is presented in Figure 6, and the most relevant metric parameters are reported in the corresponding legend. Crystal data and structural refinement details are presented in Table 3.

As can be seen, the structure of **8** is totally different from that of dimer **7**. Complex **8** is a trinuclear palladium complex that features two DMP-xantphos units. Each unit behaves as an eight-electron donor. The two phosphorus atoms are η^1-coordinated on the central palladium atom, whereas one of the two phospholes also behaves as a four-electron donor through its two double bonds, which are η^2-coordinated to two different Pd-Cl fragments. Thus, two Pd-Cl fragments are encapsulated by two phosphole rings that lie in two perpendicular planes. Mathey and co-workers already reported the ability of the 3,4-dimethylphospholyl unit to coordinate a metal atom through both the phosphorus and the diene system in the synthesis of a dinuclear cobalt complex containing two 3,4-dimethylphospholyl units.[31] In this complex each cobalt is coordinated to the two double bonds of one phosphole ring and to the phosphorus atom of the second ring. Complex **8** on the other hand is, to the best of our knowledge, the first complex where two metal atoms are sandwiched between two phospholes coordinated exclusively through the π system.

This particular arrangement raises a problem for the electron counting in **8**. If eight electrons are given by the four phosphorus atoms to the central palladium atom and four electrons to the two [PdCl] fragments, complex **8** is a 50-electron complex that features one zerovalent palladium atom and a dimeric Pd^I unit. In this unit, each palladium atom is surrounded by 16 electrons, six donated by the ligands and one electron residing in a Pd2−Pd2′ bond. Not surprisingly, this Pd2−Pd2′ (2.5759(8) Å) bond is significantly shorter than the Pd2−Pd1 and Pd2′−Pd1 bonds

(31) Holand, S.; Mathey, F.; Fischer, J.; Mitschler, A. *Organometallics* **1983**, *2*, 1234−1238.

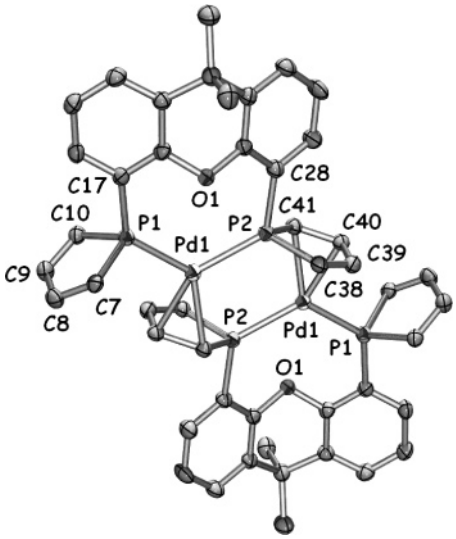

Figure 5. View of one molecule of **7**. The numbering is arbitrary and different from that used in NMR spectra. Thermal ellipsoids are drawn at the 30% probability level. Hydrogen atoms and phenyl groups on phosphole have been omitted for clarity. Selected bond distances (Å) and angles (deg): P(1)−C(17), 1.829(3); P(2)−C(28), 1.865(3); P(1)−C(10), 1.818(3); C(9)−C(10), 1.353(5); C(8)−C(9), 1.442(5); C(7)−C(8), 1.360(5); P(1)−C(7), 1.822(3); Pd(1)−P(1), 2.309(1); Pd(1)−P(2), 2.335(1); P(2)−C(38), 1.844(3); C(38)−C(39), 1.343(5); C(39)−C(40), 1.462(5); C(40)−C(41), 1.435(4); P(2)−C(41), 1.826(3); Pd(1)−C(40), 2.151(3); Pd(1)−C(41), 2.234-(3); Pd(1)−Pd(2), 4.03(1); C(17)−P(1)−Pd(1), 128.5(1); C(28)−P(2)−Pd(1), 123.1(1); C(10)−P(1)−C(7), 91.3(2); C(41)−P(2)−C(38), 90.9(2); P(1)−Pd(1)−P(2), 120.60(4); C(40)−Pd(1)−P(1), 95.3(1); C(41)−Pd(1)−P(1), 129.6(1); C(40)−Pd(1)−P(2), 143.9-(1); C(41)−Pd(1)−P(2), 108.6(1).

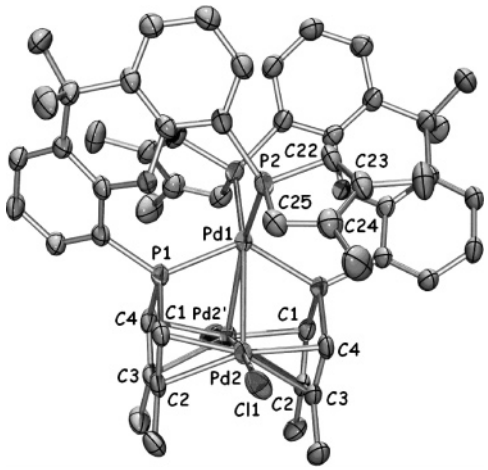

Figure 6. View of one molecule of **8**. The numbering is arbitrary and different from that used in NMR spectra. Thermal ellipsoids are drawn at the 30% probability level. Hydrogen atoms are omitted for clarity. Selected bond distances (Å) and angles (deg): Pd(1)−P(1), 2.317(1); Pd(1)−P(2), 2.397(1); Pd(1)−Pd(2), 2.8499(7); P(1)−C(1), 1.789(4); C(1)−C(2), 1.419(5); C(2)−C(3), 1.452(6); C(3)−C(4), 1.403(5); P(1)−C(4), 1.795(4); Pd(2)−C(1), 2.159(3); Pd(2)−C(2), 2.321(3); Pd(2)−C(3), 2.329(3); Pd(2)−C(4), 2.149-(3); Pd(2)−Cl(1), 2.406(1); Pd(2)-Pd(2′), 2.5759(8); P(2)−C(22), 1.787(3); C(22)−C(23), 1.350(5); C(23)−C(24), 1.479(6); C(24)−C(25), 1.364(5); P(2)−C(25), 1.783(4); P(1)−Pd(1)−P(1), 129.56-(5); P(2)−Pd(1)−P(2), 99.00(5); Pd(2′)−Pd(1)−Pd(2), 53.73(2); Pd(2′)−Pd(2)−Pd(1), 63.13(1).

(2.8499(7) Å). This led us to conclude that no bonding occurs between the central palladium atom and the two [Pd-Cl] fragments.

Table 4. Allylation of Aniline Using Catalysts 5, 6, and 7

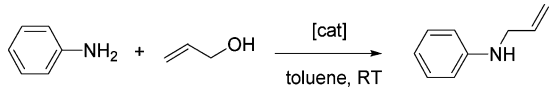

entry	catalyst (mol %)[a]	additive	time (h)	conversion (%)
1	**5OTf** (1 mol %)	no	1	100
2	**6OTf** (1 mol %)	no	1	15
3	**5OTf** (0.1 mol %)	no	2	73
4	**5OTf** (0.1 mol %)	$MgSO_4$	1	95
5	**7** (0.05 mol %)	no	5	54
6	**7** (0.05 mol %)	NH_4Br	5	75

[a] Reactions conditions: 2 mmol of C_3H_6O, 4 mmol of $PhNH_2$, toluene (4 mL). After the reaction time indicated, conversions were determined by GC with internal standard and correction factors.

Scheme 7. Synthesis of Dimer 8

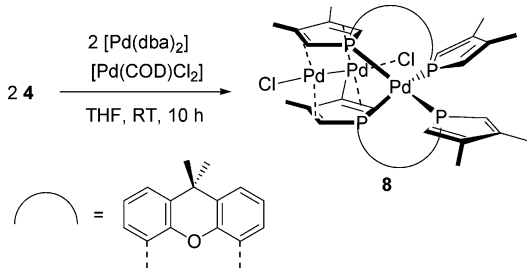

Scheme 8. Energetic Variation of the LUMO of a PdL_2(allyl) Complex as a Function of the L−Pd−L Angle

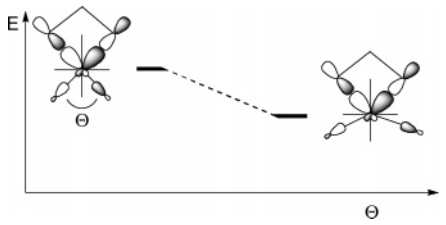

No mechanism accounting for the formation of **8** can be proposed at this stage. In order to devise a more straightforward approach to this interesting species, a new synthetic procedure was developed. Since one can reason that complex **8** formally results from the reaction of 2 equiv of ligand **2** with two palladium(0) and one palladium(II), 2 equiv of $[Pd(dba)_2]$ and 1 equiv of $[Pd(COD)Cl_2]$ were reacted with 2 equiv of **2** in THF at room temperature. After stirring for 10 h, complex **8** was the sole species detected in the ^{31}P NMR spectrum of the reaction mixture. By removing the solvent *in vacuo* and washing the resulting solid with diethyl ether, **8** was isolated in 85% yield as a brown solid, which could be fully characterized by means of NMR spectroscopy and elemental analysis (Scheme 7).

3. Catalytic Activity of Complexes 5, 6, 7, and 8. The catalytic activity of complexes **5**−**8** was evaluated in the palladium-catalyzed allylation of primary amines using aniline as nucleophile (commonly employed to test the activity of a catalyst in this process[24,32]). In a first series of experiments, catalytic amounts of complexes **5OTf** and **6OTf** (1%) were reacted with allyl alcohol (1 equiv) in the presence of aniline (2 equiv) in toluene at room temperature. Under these conditions, a complete conversion was observed with complex **5OTf** in 1 h, whereas complex **6OTf** exhibited a low activity (15%

(32) Ozawa, F.; Okamoto, H.; Kawagishi, S.; Yamamoto, S.; Minami, T.; Yoshifuji, M. *J. Am. Chem. Soc.* **2002**, *124*, 10968−10969.

Table 3. Crystal Data and Structural Refinement Details for Complexes 7 and 8

	7	**8**
cryst size [mm]	0.14 × 0.12 × 0.06	0.16 × 0.10 × 0.10
empirical formula	$C_{94}H_{72}O_2P_4Pd_24(CH_2Cl_2)$	$C_{54}H_{56}Cl_2O_2P_4Pd_3C_4H_8O$
molecular mass	954.95	697.59
cryst syst	triclinic	monoclinic
space group	$P\bar{1}$	$C2/c$
a [Å]	13.057(1)	17.642(1)
b [Å]	13.211(1)	19.869(1)
c [Å]	15.355(1)	16.475(1)
α [deg]	94.885(1)	90.00
β [deg]	111.473(1)	92.641(1)
γ [deg]	117.498(1)	90.00
V [Å]^3	2080.1(13)	5769(3)
Z	2	8
calcd density [g·cm^{-3}]	1.525	1.606
abs coeff [cm^{-1}]	0.818	1.176
θ_{max} [deg]	26.37	28.70
F(000)	972	2832
index ranges	−15 16; −16 16; −19 19	−23 23; −23 26; −22 22
no. of reflns collected/indep	25 609/8483	12 426/7423
no. of reflns used	6347	5369
R_{int}	0.0439	0.0216
abs corr	0.8940 min., 0.9525 max.	0.8341 min., 0.8914 max.
no. of params refined	516	300
refln/param	12	17
final R1[a]/wR2 [$I > 2\sigma(I)$] [b]	0.0402/0.0402	0.0421/0.1249
goodness-of-fit on F^2	1.026	1.034
diff peak/hole [e·Å^{-3}]	1.007(0.081)/−0.797(0.081)	1.231(0.115)/−0.983(0.115)

[a] $R1 = \sum||F_o| - |F_c||/\sum|F_o|$. [b] $wR2 = (\sum w||F_o| - |F_c||^2/\sum w|F_o|^2)^{1/2}$.

Scheme 9. Activation Energies Needed for the Dissociation of the Phenylallylammonium Ligand to Produce [Pd(3)] and [Pd(dppe)] Complexes (energies in kcal/mol)

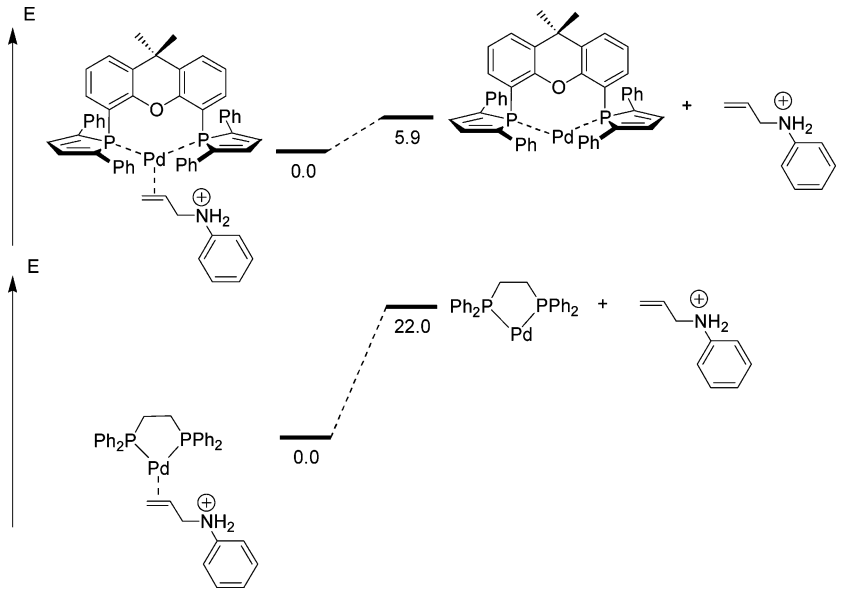

conversion after 1 h and 30% after 5 h) (see Table 4, entries 1 and 2). Further experiments were carried out with complex **5OTf** where the catalyst load was reduced to 0.1% (entry 3). Even at such low catalyst loading, the activity of **5OTf** remained very good. Even more satisfying results were obtained when a water scavenger, such as $MgSO_4$, was used with 0.1% of catalyst. In this case a near complete conversion was obtained after 1 h at room temperature (entry 4), which compares favorably with the best catalytic systems developed so far.[32] On the basis of the fact that we recently demonstrated a 14-VE PdL_2 complex to be the active species,[24] additional experiments were carried out using dimer **7**. In solution this dimer may dissociate to give two 14-VE [Pd(DPP)] monomers. Results of these experiments are also reported in Table 4. Experiments were conducted with 0.05% of **7** under the same experimental conditions. As expected, **7** was found to be less active than its allyl precursor. Clearly, dissociation into a monomeric form is not favored. Nevertheless, a conversion of 54% was obtained after 5 h (entry 5). Interestingly, we found that the presence of NH_4Br (5 mol %) as cocatalyst yielded better conversion yields. This observation is in good agreement with the proposed mechanism, showing that the allylammonium produced during the reaction assists the elimination of water from a transient [$L_2Pd(\eta^2$-allylalcohol)] complex.[24] In the presence of NH_4Br, a 75% conversion yield was obtained after 5 h at room temperature (entry 6). Experiments conducted with dimer **8** under the same experimental conditions lead to poor conversions. The *in-situ* formation of complex **8** during catalysis with complex **6** may help explain why complex **6** displays such poor activity.

Two factors explain the remarkable activity of complex **5**: the strong π-accepting capacity of the diphenylphosphole unit and the wide P−Pd−P bite angle. Both effects work in the same direction. In 1996, on the basis of computational results, Szabo concluded that nucleophilic attack at the terminal carbon atom of the allyl is favored by an increase of the bite angle.[33] These conclusions were experimentally confirmed by Kamer and co-workers, who evaluated a series of diphosphines in the palladium-catalyzed allylation,[11] and further confirmed very recently by Hartwig and co-workers for a comparable catalytic transformation.[9] There is a vacant antibonding MO resulting from the combination of a vacant nonbonding d_{xy} orbital of the metal with the n_π MO of the allyl ligand, featuring important contributions at the terminal carbons. Increasing the bite angle of a ligand surrounding the palladium results in the stabilization of this antibonding MO (Scheme 8). The presence of strong π-accepting ligands further contributes to lowering the energy of the vacant nonbonding d_{xy} orbital. Therefore, both the bite angle and the π-accepting capacity of the ligand reduces the palladium−allyl bond strength and favors nucleophilic attack at the terminal carbon.

Recent DFT calculations have also demonstrated that the rate-limiting step in this coupling process is the release of the η^2-allylammonium ligand, formed by nucleophilic attack of the amine onto the allyl ligand, resulting in the formation of a 14-VE PdL_2 fragment.[24] In order to get further insight into the reactivity of complex **5**, DFT calculations were carried out to estimate the activation energy needed for this decomplexation process. A comparison was made with the corresponding [Pd(dppe)] (dppe = 1,2-bis-diphenylphosphinoethane) complex, which is known to act as a relatively poor catalyst (20% conversion yield after 24 h using 1% of catalyst[23]). These calculations were carried out within the framework of DFT with the Gaussian 03W set of programs. Due to the size of the system, the ONIOM method combining the B3PW91 with the UFF force field was employed. The phenyl groups of the phosphole ligands, those of the dppe ligand, and that of the aniline were computed at the molecular mechanic level, but single-point calculations on the optimized structure were carried out at the DFT level using the polarized continuum model (PCM) (solvent = THF). Further details (used basis sets) regarding this computational part of the study are presented in the Experimental Section. As expected, these calculations revealed that decomplexation of the allylammonium moiety is by far easier ($\Delta G^{\pm} = 5.9$ kcal/mol) in the case of complex **5** than in the corresponding dppe complex ($\Delta G^{\pm} = 22.0$ kcal/mol) (Scheme 9). This important difference is accounted for by the stronger π-accepting capacity of the DBP-xantphos ligand with regard to dppe.

Conclusions

Two new phosphole-xanthene derivatives, DPP-Xantphos **3** and DMP-Xantphos **4**, have been synthesized. Although, both ligands can behave as a chelator for a [Pd(allyl)] fragment, their respective stability strongly depends on the nature of the counteranion employed. Whereas triflate derivatives, **5OTf** and **6OTf**, were found to be stable, decomposition occurs when chloride is used as counteranion. As a result, two unusual structures could be characterized, a dimeric 32-VE palladium(0) complex resulting from the decomposition of **5Cl** and a trinuclear species featuring two 16-VE palladium(I) and one 18-VE palladium(0) fragment resulting from the decomposition of **6Cl**. Examination of the X-ray data of **5OTf** and **6OTf** suggests that the reactivity of both complexes is mainly governed by the substitution pattern of the phosphole units, dictating the structure of the complexes. The presence of phenyl substituents at the 2-positions of the phospholes forces the complex to adopt a geometry with a relatively large P−Pd−P bite angle. In good agreement with previous studies, this leads complex **5OTf** to be highly reactive toward nucleophilic attacks at the allyl ligand by C and N nucleophiles. Therefore, complex **5OTf** exhibits high catalytic activity in the allylation of aniline. This high catalytic activity results from the combination of two effects: a large bite angle at palladium, which enhances the reactivity of the allyl ligand, and the strong π-accepting capacity of the diphenylphosphole units, which favors the formation of a 14-VE palladium(0) complex. Further experiments, which are currently underway in our laboratories, will now focus on a systematic investigation of the coordination chemistry of these new ligands and their use in catalytic processes of synthetic relevance.

Experimental Section

Computational Details. Calculations were performed with the GAUSSIAN 03 series of programs.[34] Geometries were optimized with the ONIOM method using a combination of the B3PW91 functional[35,36] with the UFF force field.[37] Phenyl groups of the phosphole ring in DPP-Xantphos and aniline, as well as phenyl groups of the dppe ligands, were calculated at the molecular mechanics level. The other atoms were calculated at the quantum level of theory. The standard 6-31G* basis set was used for all atoms (H, C, N, O, and P). The basis set used for metals (Pd) is the Hay and Wadt[38] small-core quasi-relativistic effective core potential with the double-ζ valence basis set (441s/2111p/311d) augmented with a f-polarization function (exponent = 1.472).[39] Minima were characterized by frequencies calculation. Single-point calculations were performed on all optimized geometries at the quantum level for all atoms using the PCM-UFF model.[40−43]

Synthesis. All reactions were routinely performed under an inert atmosphere of argon or nitrogen using Schlenk and glovebox techniques and dry, deoxygenated solvents. Dry hexanes were

(33) Szabo, K. J. *Organometallics* **1996**, *15*, 1128−1133.

(34) Frisch, M. J.; Trucks, G. W.; Schlegel, H. B.; Scuseria, G. E.; Robb, M. A.; Cheeseman, J. R.; Montgomery, J. A.; Vreven, T.; Kudin, K. N.; Burant, J. C.; Millam, J. M.; Iyengar, S. S.; Tomasi, J.; Barone, V.; Mennucci, B.; Cossi, M.; Scalmani, G.; Rega, N.; Petersson, G. A.; Nakatsuji, H.; Hada, M.; Ehara, M.; Toyota, K.; Fukuda, R.; Hasegawa, J.; Ishida, M.; Nakajima, T.; Honda, Y.; Kitao, O.; Nakai, H.; Klene, M.; Li, X.; Knox, J. E.; Hratchian, H. P.; Cross, J. B.; Adamo, C.; Jaramillo, J.; Gomperts, R.; Stratmann, R. E.; Yazyev, O.; Austin, A. J.; Cammi, R.; Pomelli, C.; Ochterski, J. W.; Ayala, P. Y.; Morokuma, K.; Voth, G. A.; Salvador, P.; Dannenberg, J. J.; Zakrzewski, V. G.; Dapprich, S.; Daniels, A. D.; Strain, M. C.; Farkas, O.; Malick, D. K.; Rabuck, A. D.; Raghavachari, K.; Foresman, J. B.; Ortiz, J. V.; Cui, Q.; Baboul, A. G.; Clifford, S.; Cioslowski, J.; Stefanov, B. B.; Liu, G.; Liashenko, A.; Piskorz, P.; Komaromi, I.; Martin, R. L.; Fox, D. J.; Keith, T.; Al-Laham, M. A.; Peng, C. Y.; Nanayakkara, A.; Challacombe, M.; Gill, P. M. W.; Johnson, B.; Chen, W.; Wong, M. W.; Gonzalez, C.; Pople, J. A. *GAUSSIAN 03*, Revision B.04; Gaussian, Inc.: Pittsburgh, PA, 2003.

(35) Becke, A. D. J. *Phys. Chem.* **1993**, *98*, 5648−5662.

(36) Perdew, J. P.; Wang, Y.; *Phys. Rev. B* **1992**, *45*, 13244−13249.

(37) Rappe, A. K.; Kasewit, C. J.; Colwell, K. S.; Goddard, W. A., III; Skiff, W. M. *J. Am. Chem. Soc.* **1992**, *114*, 10024.

(38) Hay, P. J.; Wadt, W. R. *J. Chem. Phys.* **1985**, *82*, 299−310.

(39) Ehlers, A. W.; Böhme, M.; Dapprich, A.; Gobbi, A.; Höllwarth, A.; Jonas, V.; Köhler, K. F.; Stegmann, R.; Veldkamp, A.; Frenking, G. *Chem. Phys. Lett.* **1993**, *208*, 111−114.

(40) Miertus, S.; Scrocco, E.; Tomasi, J. *Chem. Phys.* **1981**, *55*, 117.

(41) Barone, V.; Cammi, R.; Tomasi, J. *Chem. Phys. Lett.* **1996**, *255*, 327.

(42) Cossi, M.; Scalmani, G.; Rega, N.; Barone, V. *J. Chem. Phys.* **2002**, *117*, 43−54.

(43) Barone, V.; Improta, R.; Rega, N. *Theor. Chem. Acc.* **2004**, *111*, 237−245.

obtained by distillation from Na/benzophenone. Dry dichloromethane was distilled on P_2O_5, dry triethylamine on KOH, and dry toluene on metallic Na. Nuclear magnetic resonance spectra were recorded on a Bruker AC-300 SY spectrometer operating at 300.0 MHz for ^{1}H, 75.5 MHz for ^{13}C, and 121.5 MHz for ^{31}P. Solvent peaks are used as internal reference relative to Me_4Si for ^{1}H and ^{13}C chemical shifts (ppm); ^{31}P chemical shifts are relative to a 85% H_3PO_4 external reference. Coupling constants are given in hertz. The following abbreviations are used: s, singlet; d, doublet; t, triplet; m, multiplet. 1,2,5-Triphenylphosphole is easily available on a multigram scale from the simple reaction of dichlorophenylphosphine with 1,4-diphenyl-1,3-butadiene.[44] All other reagents and chemicals were obtained commercially and used as received. Elemental analyses were performed by the "Service d'analyse du CNRS", at Gif sur Yvette, France. The GC yields were determined on a Perichrom 2100 gas chromatograph equipped with a Perichrom column (silicone OV1, CP-SIL 5 CB), 30 m × 0.22 mm.

Synthesis of Cyanophosphole 1. To a solution of 1,2,5-triphenylphosphole (5.0 g, 16 mmol) in tetrahydrofuran (100 mL) cooled to 0 °C was added lithium wire (0.25 g, 65 mmol), and the mixture was stirred at 0 °C for 2 h. $AlCl_3$ (0.35 g, 2.65 mmol) was added, and the mixture was stirred at 0 °C for 1 h and cannulated on a solution of BrCN (3.4 g, 32 mmol) in tetrahydrofuran (50 mL) at −78 °C. The mixture was then allowed to warm slowly to room temperature. The solvent was removed and replaced by dichloromethane. The solution obtained was filtered off on silica gel, dichloromethane was removed, and the solid obtained was triturated with Et_2O to afford a yellow powder (2.1−2.4 g, 70%). Anal. Calcd for $C_{17}H_{12}NP$: C, 78.15; H, 4.63. Found: C, 78.00; H, 4.73. ^{31}P{^{1}H} NMR ($CDCl_3$): δ −49.0 (s). ^{1}H NMR ($CDCl_3$): δ 7.18−7.32 (m, 8H, $H_{aromatic}$ and $H_{\beta-phosphole}$), 7.47 (d, $^3J_{HH}$ = 7.9 Hz, 4H, $H_{ortho-phenyl}$). ^{13}C NMR ($CDCl_3$): δ 116.5 (d, $^2J_{CP}$ = 74.4 Hz, C_{CN}), 126.5 (d, $^3J_{CP}$ = 9.2 Hz, $C_{ortho-phenyl}$), 128.5 ($C_{para-phenyl}$), 129 ($C_{meta-phenyl}$), 133.5 (d, $^2J_{CP}$ = 16.8 Hz, $C_{ipso-phenyl}$), 136.5 (d, $^2J_{CP}$ = 16.8 Hz, $C_{\beta-phosphole}$), 142.5 ($C_{\alpha-phosphole}$).

Synthesis of DPP-Xantphos 3. To a solution of 9,9′-dimethylxanthene (1.0 g, 4.8 mmol) and TMEDA (2.1 mL, 14 mmol) in Et_2O (45 mL) at −78 °C was added a 1.4 M solution of *sec*-butyllithium in cyclohexane (10 mL, 14 mmol). The reaction mixture was stirred at room temperature for 20 h. Two equivalents of cyanophosphole **1** (2.6 g, 9.6 mmol) was added slowly at −78 °C. The mixture was allowed to warm to room temperature and was stirred for 3 h. The title compound, which precipitated, was filtered off and dissolved in dichloromethane, and the solution was filtered off on silica gel. The solvent was removed and the compound recrystallized from Et_2O to afford a yellow solid (1.6−2.1 g, 65%). Anal. Calcd for $C_{47}H_{36}OP_2$: C, 83.17; H, 5.35. Found: C, 83.13; H, 5.36. ^{31}P{^{1}H} NMR (CD_2Cl_2): δ −17.0 (s). ^{1}H NMR (CD_2Cl_2): δ 1.42 (s, 6H, CH_3), 6.71 (m, 2H, C$H_{xanthene}$), 6.80 (t, $^3J_{HH}$ = 7.6 Hz, 2H, C$H_{xanthene}$), 7.03−7.19 (m, 12H, $H_{aromatic}$), 7.22−7.32 (m, 6H, $H_{aromatic}$ and $H_{\beta-phosphole}$), 7.63 (d, 8H, $^3J_{HH}$ = 7.3 Hz, $H_{ortho-phenyl}$). ^{13}C NMR (CD_2Cl_2): δ 32.0 (*C*H_3), 36.0 (*C*$(CH_3)_2$), 118.5 (vt, $\sum J$ = 11.6 Hz, *C*P), 124.5 (*C*$H_{xanthene}$), 127.0 (vt, $\sum J$= 5.0 Hz, $C_{aromatic}$), 128.0 ($C_{aromatic}$), 128.5 (*C*$H_{xanthene}$), 129.5 ($C_{aromatic}$), 132.5 ($C_{aromatic}$), 132.5 (*C*$H_{xanthene}$), 133.5 (vt, $\sum J$ = 5.1 Hz, $C_{\beta-phosphole}$), 137.0 (vt, $\sum J$ = 8.5 Hz, $C_{aromatic}$), 154.5 ($C_{\alpha-phosphole}$), 155.0 (vt, $\sum J$ = 11.5 Hz, *C*O).

Synthesis of DMP-Xantphos 4. To a solution of 9,9′-dimethylxanthene (1.0 g, 4.8 mmol) and TMEDA (2.1 mL, 14 mmol) in Et_2O (45 mL) at −78 °C was added a 1.4 M solution of *sec*-butyllithium in cyclohexane (10 mL, 14 mmol). The reaction mixture was stirred at room temperature for 20 h. Two equivalents of cyanophosphole **2** (1.3 g, 9.6 mmol) was added slowly at −78 °C. The mixture was allowed to warm to room temperature and was stirred for 3 h. The title compound, which precipitated, was filtered off and dissolved in dichloromethane, and the solution was filtered off on silica gel. The solvent was removed and the compound recrystallized from Et_2O to afford a white solid (1.0−1.15 g, 55%). Anal. Calcd for $C_{27}H_{28}OP_2$: C, 75.34; H, 6.56. Found: C, 75.26; H, 6.60. ^{31}P{^{1}H} NMR (CD_2Cl_2): δ −9.5 (s). ^{1}H NMR (CD_2Cl_2): δ 1.51 (s, 6H, C(CH_3)$_2$), 2.02 (d, $^4J_{HP}$ = 3.4 Hz, 12H, C═CCH_3), 6.78 (d, 4H, $^2J_{HP}$ = 36.4 Hz, $H_{\alpha-phosphole}$), 6.88 (t, $^3J_{HH}$ = 7.7 Hz, 2H, C$H_{xanthene}$), 7.03 (m, $\sum J$ = 13.3 Hz, 2H, C$H_{xanthene}$), 7.20 (dd, $^3J_{HH}$ = 7.8 Hz, $^4J_{HH}$ = 1.3 Hz, 2H, C$H_{xanthene}$). ^{13}C NMR (CD_2Cl_2): δ 16.0 (vt, $\sum J$ = 3.4 Hz, C═C*C*H_3), 30.5 (C(*C*H_3)$_2$), 32.5 (*C*$(CH_3)_2$), 121.0 (m, $\sum J$ = 15.9 Hz, *C*P), 122.0 (*C*$H_{xanthene}$), 124.5 (*C*$H_{xanthene}$), 125.5 (d, $^1J_{C-P}$ = 2.1 Hz, $C_{\alpha-phosphole}$), 128.5 (*C*$C(CH_3)_2$), 128.5 (*C*$H_{xanthene}$), 147.0 (m, $\sum J$ = 22.5 Hz, $C_{\beta-phosphole}$), 149.0 (m, $\sum J$ = 15.3 Hz, *C*O).

Synthesis of Complex 5, [Pd(C_3H_5)(3)][OTf]. To a solution of DPP-Xantphos **3** (100 mg, 0.15 mmol) in dichloromethane (3 mL) was added $[Pd_2(\mu\text{-}Cl)_2(C_3H_5)_2]$ (27 mg, 0.075 mmol) at room temperature. The solution was stirred for 5 min. Completion of the reaction was confirmed by ^{31}P NMR. Silver triflate salt (38 mg, 0.15 mmol) was then added to the solution at room temperature. The mixture was stirred 15 min, filtered, and concentrated, to afford a yellow-green solid (140 mg, 95%). Anal. Calcd for $C_{51}H_{41}F_3O_4P_2PdS$: C, 62.81; H, 4.24. Found: C, 62.68; H, 4.23. ^{31}P{^{1}H} NMR (CD_2Cl_2): δ −0.5 (s). ^{1}H NMR (CD_2Cl_2): δ 1.58 (s, 3H, C(CH_3)$_2$), 1.63 (s, 3H, C(CH_3)$_2$), 3.30 (dd, 2H, $^3J_{HH}$ = 13.4 Hz, $^4J_{HP}$ = 7.8 Hz, H_{allyl}), 3.95 (d, $^3J_{HH}$ = 7.1 Hz, 2H, H_{allyl}), 5.50 (vsept, $\sum J$ = 41.3 Hz, 1H, H_{allyl}), 7.13−7.32 (m, 16H, $H_{aromatic}$), 7.48−7.63 (m, 14H, $H_{aromatic}$). ^{13}C NMR (CD_2Cl_2, 25 °C): δ 27.0 (C(*C*H_3)$_2$), 27.5 (C(*C*H_3)$_2$), 37.5 (*C*$(CH_3)_2$), 82.5 (vt, $\sum J$ = 23.7 Hz, *C*H_{allyl}), 111.0 (*C*H_{allyl}), 122.5 ($C_{aromatic}$), 126.5 ($C_{aromatic}$), 127.1 ($C_{aromatic}$), 127.3 ($C_{aromatic}$), 129.3 ($C_{aromatic}$), 129.5 ($C_{aromatic}$), 129.7 ($C_{aromatic}$), 129.8 ($C_{aromatic}$), 129.9 ($C_{aromatic}$), 130.0 ($C_{aromatic}$), 133.4 (vt, $\sum J$ = 14.6 Hz, *C*P), 135.0 (vt, $\sum J$ = 12.2 Hz, $C_{\beta-phosphole}$), 135.4 (vt, $\sum J$ = 12.2 Hz, $C_{\beta-phosphole}$), 136.6 (vt, $\sum J$ = 4.6 Hz, $C_{aromatic}$), 148.2 (AXX′, $\sum J$ = 57.9 Hz, $C_{\alpha-phosphole}$), 149.5 (AXX′, $\sum J$ = 57.9 Hz, $C_{\alpha-phosphole}$), 157.1 (vt, $\sum J$ = 9.5 Hz, *C*O).

Synthesis of Complex 6, [Pd(4)(C_3H_5)$_2$][OTf]. To a solution of DMP-Xantphos **4** (100 mg, 0.23 mmol) in dichloromethane (3 mL) was added $[Pd_2(\mu\text{-}Cl)_2(C_3H_5)_2]$ (43 mg, 0.12 mmol) at room temperature. The solution was stirred for 5 min. Completion of the reaction was confirmed by ^{31}P NMR. Silver triflate salt (60 mg, 0.23 mmol) was then added to the solution at room temperature. The mixture was stirred 15 min, filtered, and concentrated, to afford a white-gray solid (160 mg, 92%). Anal. Calcd for $C_{31}H_{33}F_3O_4P_2PdS$: C, 51.21; H, 4.58. Found: C, 51.13; H, 4.57. ^{31}P{^{1}H} NMR (CD_2Cl_2): δ 4.45 (s). ^{1}H NMR(CD_2Cl_2): δ 1.65 (s, 6H, C(CH_3)$_2$), 2.24 (s, 12H, C═CCH_3), 3.11 (dd, 2H, $^3J_{HH}$ = 13.4 Hz, $^3J_{HP}$ = 9 Hz, H_{allyl}), 4.78 (dd, $^3J_{HH}$ = 7.2 Hz, $^4J_{HP}$ = 2.8 Hz, 2H, H_{allyl}), 5.27 (vsept, $\sum J$ = 41.6 Hz, 1H, H_{allyl}), 6.77 (d, $^2J_{HP}$ = 7.8 Hz, 2H, $H_{\alpha-phosphole}$), 6.80 (d, $^2J_{HP}$ = 7.8 Hz, 2H, $H_{\alpha-phosphole}$), 7.19−7.29 (m, 4H, C$H_{xanthene}$), 7.57 (dd, 2H, $^3J_{HH}$ = 6.0 Hz, $^3J_{HH}$ = 2.0 Hz, C$H_{xanthene}$). ^{13}C NMR (CD_2Cl_2, 25 °C): δ 18.3 (vt, $^3J_{CP}$ = 6.1 Hz, C═C*C*H_3), 27.4 (C(*C*H_3)$_2$), 27.6 (C(*C*H_3)$_2$), 37.0 (*C*$(CH_3)_2$), 72.9 (vt, $\sum J$ = 28.0 Hz, *C*H_{allyl}), 117.3 (dd, $^1J_{CP}$ = 23.0 Hz, $^3J_{CP}$ = 21.7 Hz, *C*P), 120.6 (t, $^3J_{CP}$ = 4.8 Hz, *C*H_{allyl}), 123.0 (dd, $^1J_{CP}$ = 25.0 Hz, $^3J_{CP}$ = 22.4 Hz, $C_{\alpha-phosphole}$), 123.6 (dd, $^1J_{CP}$ = 20.9 Hz, $^3J_{CP}$ = 18.3 Hz, $C_{\alpha-phosphole}$), 126.0 (vt, $\sum J$ = 7.8 Hz, *C*$H_{xanthene}$), 128.5 (*C*$H_{xanthene}$), 129.2 (*C*$H_{xanthene}$), 135.4 (vt, $\sum J$ = 4.2 Hz, *C*$C(CH_3)_2$), 155.1 (vt, $\sum J$ = 10.0 Hz, $C_{\beta-phosphole}$), 155.4 (vt, $\sum J$ = 10.0 Hz, $C_{\beta-phosphole}$), 155.6 (vt, $\sum J$ = 4.2 Hz, *C*O).

Synthesis of Complex 7, [Pd$_2$(3)$_2$]. To a solution of DPP-Xantphos **3** (100 mg, 0.147 mmol) in dichloromethane (3 mL) was added $[Pd_2(\mu\text{-}Cl)_2(C_3H_5)_2]$ (27 mg, 0.074 mmol) at room temperature. The solution turned from yellow to orange and was stirred for 5 min. Completion of the reaction was confirmed by ^{31}P NMR. Aniline (100 μL, 1.1 mmol) was then added to the solution at room temperature. A red-brown, insoluble solid appeared, which was

(44) Campbell, I. G.; Cookson, R. C.; Hocking, M. B.; Hughes, A. N. *J. Chem. Soc.* **1965**, 2184−2193.

filtered, washed with dichloromethane, and dried (105 mg, 91%). Anal. Calcd for $C_{94}H_{72}O_2P_4Pd_2$: C, 71.90; H, 4.62. Found: C, 71.77; H, 4.62. Insolubility of the compound prevented NMR studies.

Synthesis of Complex 8, [Pd$_3$(4)$_2$Cl$_2$]. To a solution of [Pd(COD)Cl$_2$] (33 mg, 0.12 mmol) and [Pd(dba)$_2$] (130 mg, 0.24 mmol) in tetrahydrofuran (2 mL) was added the DMP-Xantphos **4** (100 mg, 0.23 mmol). After 10 h stirring, the solvent was removed and 10 mL of diethyl ether was added. The resultant brown solid was filtered off and again washed with diethyl ether (120 mg, 85%). Anal. Calcd for $C_{54}H_{56}Cl_2O_2P_4Pd_3$: C, 51.84; H, 4.51. Found: C, 51.74; H, 4.51. $^{31}P\{^1H\}$ NMR (CD_2Cl_2): δ −8.5 (t, $^2J_{PP}$ = 27.9 Hz), −4.5 (t, $^2J_{PP}$ = 27.9 Hz). ^1H NMR (CD_2Cl_2): δ 1.29 (s, 6H, C═CCH_3), 1.38 (s, 6H, C(CH_3)$_2$), 1.89 (s, 6H, C(CH_3)$_2$), 1.92 (s, 6H, C═CCH_3), 1.95 (s, 6H, C═CCH_3), 2.00 (s, 6H, C═CCH_3), 4.59 (AA′MM′XX′, $\sum J$ = 36.6 Hz, 2H, H$_{\alpha-phosphole}$), 5.15 (AA′MM′XX′, $\sum J$ = 31.8 Hz, 2H, H$_{\alpha-phosphole}$), 5.59 (AA′MM′XX′, $\sum J$ = 31.8 Hz, 2H, H$_{\alpha-phosphole}$), 6.36 (ddd, $^3J_{HH}$ = 7.8 Hz, $^2J_{HP}$ = 6.6 Hz, $^4J_{HH}$ = 1.2 Hz, 2H, H$_{aromatic}$), 6.65 (AA′MM′XX′, $\sum J$ = 36.6 Hz, 2H, H$_{\alpha-phosphole}$), 6.84 (t, 2H, $^3J_{HH}$ = 7.8 Hz, H$_{aromatic}$), 7.14−7.23 (m, 4H, H$_{aromatic}$), 7.38 (dd, $^3J_{HH}$ = 7.8 Hz, $^4J_{HH}$ = 1.2 Hz, 2H, H$_{aromatic}$), 7.56 (dd, $^3J_{HH}$ = 7.5 Hz, $^4J_{HH}$ = 1.8 Hz, 2H, H$_{aromatic}$). ^{13}C NMR (CD_2Cl_2, 25 °C): δ 17.0 (C═CCH_3), 17.8 (d, J_{CP} = 3.7 Hz, C═CCH_3), 18.0 (d, J_{CP} = 4.2 Hz, C═CCH_3), 23.7 (C(*C*H$_3$)$_2$), 32.2 (C(*C*H$_3$)$_2$), 37.1 (*C*(CH$_3$)$_2$), 65.2 (vt, $\sum J$ = 29.6 Hz, C$_{\alpha-phosphole}$), 70.0 (vt, $\sum J$ = 27.8 Hz, C$_{\alpha-phosphole}$), 103.7 (vt, $\sum J$ = 12.0 Hz, C$_{\beta-phosphole}$), 106.0 (vt, $\sum J$ = 13.2 Hz, C$_{\beta-phosphole}$), 124.3 (C$_{aromatic}$), 124.9 (C$_{aromatic}$), 125.4 (vt, $\sum J$ = 6.9 Hz, C$_{\alpha-phosphole}$), 127.2 (C$_{aromatic}$), 127.8 (C$_{aromatic}$), 128.9 (C$_{aromatic}$), 129.5 (C$_{aromatic}$), 130.8 (m, C$_{\alpha-phosphole}$), 134.2 (m, *C*C(CH$_3$)$_2$), 135.9 (m, *C*C(CH$_3$)$_2$), 145.3 (vt, $\sum J$ = 11.1 Hz, C$_{\beta-phosphole}$), 149.8 (vt, $\sum J$ = 10.2 Hz, C$_{\beta-phosphole}$), 155.8 (vt, $\sum J$ = 10.8 Hz, C$_{aromatic}$), 157.0 (vt, $\sum J$ = 9.9 Hz, C$_{aromatic}$).

X-ray Crystallography for 3, 5, 6, 7, and 8. Yellow needles of **3** and **5**, white needles of **6**, and red-brown blocks of **8** crystallized by slow diffusion of hexanes into a saturated dichloromethane solution of respectively **3**, **5**, **6**, and **8**. Dark red needles of complex **7** were obtained by diffusing a solution of aniline in 1 mol/L hexanes at 4 °C into a dichloromethane solution of complex **5**. Data were collected on a Nonius Kappa CCD diffractometer using a Mo Kα (λ = 0.71073 Å) X-ray source and a graphite monochromator at 150 K. Experimental details are described in Tables 1, 2, and 3. The crystal structures were solved using SIR 97[45] and SHELXL97.[46] ORTEP drawings were made using ORTEP III for Windows.[47]

General Procedure for the Allylation of Aniline. The catalyst (19 mg of **5**, 15 mg of **6** for 1% (Table 4, entries 1 and 2); 1.9 mg of **5** for 0.1% (Table 4, entries 3 and 4); 1.6 mg of **7** for 0.05% of dimer (Table 4, entries 5 and 6)) was placed in a Schlenck tube with or without an additive as indicated in Table 4 (0.50 g of $MgSO_4$, entry 4; 10 mg of NH_4Br, entry 6) and THF (2 mL). The Schlenck tube was then filled with aniline (364 μL, 4 mmol) and allyl alcohol (136 μL, 2 mmol). The mixture was stirred at room temperature, and the progress of the reaction was monitored by GC. The mixture was filtered to remove the $MgSO_4$ and the solvent evaporated *in vacuo*. The product was then isolated by column chromatography on alumina (hexanes).

Crystallographic data can be obtained free of charge at www.ccdc.cam.ac.uk/conts/retrieving.html [or from the Cambridge Crystallographic Data Centre, 12 Union Road, Cambridge CB21EZ, UK; fax: (internat.) +44-1223/336-033; e-mail: deposit@ccdc.cam.ac.uk] with the deposition numbers CCDC 631901−631905.

Acknowledgment. The authors thank the CNRS (Centre National de la Recherche Scientifique) and the Ecole Polytechnique for the financial support of this work and IDRIS for the allowance of computer time (project no. 060616).

Supporting Information Available: Computed Cartesian coordinates, thermochemistry, and PCM energies of complexes [Pd(DBP-xantphos)(η^2-phenylallylammonium)], [Pd(DBP-xantphos)], [Pd(dppe)(η^2-phenylallylammonium)], and [Pd(dppe)]. CIF files and tables giving crystallographic data for **3**, **5OTf**, **6OTf**, **7**, and **8** (including atomic coordinates, bond lengths and angles, and anisotropic displacement parameters) and computational details. This material is available free of charge via the Internet at http://pubs.acs.org.

OM061172T

(45) Altomare, A.; Burla, M. C.; Camalli, M.; Cascarano, G.; Giacovazzo, C.; Guagliardi, A.; Moliterni, A. G. G.; Polidori, G.; Spagna, R. *SIR97*, an integrated package of computer programs for the solution and refinement of crystal structures using single-crystal data.

(46) Sheldrick, G. M. *SHELXL-97*; Universität Göttingen: Göttingen, Germany, 1997.

(47) Farrugia, L. J. *ORTEP-3*; Department of Chemistry, University of Glasgow: Scotland.